

New SWIPT Using PAPR: How It Works

Dong In Kim, Jong Ho Moon, and Jong Jin Park

Abstract—In this letter, we propose a new architecture for simultaneous wireless information and power transfer (SWIPT) which utilizes multi-sine waveforms for energy transfer and their distinct peak-to-average-power-ratios (PAPR) for information transmission. The new form of SWIPT proposed is based on an innovative idea of conveying information using the different levels of PAPR which can be measured at the output of the rectifier for energy harvesting, enabling a low-energy combined receiver. The latter is very crucial for batteryless operation of low-energy wireless devices relying much on the harvested energy. We demonstrate how the proposed idea works in terms of the information decoding via distinct PAPR, as well as the rate-energy tradeoff for a varying number of multiple tones.

Index Terms—Simultaneous wireless information and power transfer (SWIPT), multi-sine waveforms, PAPR, rate-energy tradeoffs.

I. INTRODUCTION

A BATTERY lifetime of wireless devices is becoming crucial as massive deployment of low-energy wearable devices and wireless sensors is foreseen with machine-type communication (MTC) for Internet-of-Things (IoT). To this end, a fundamental paradigm shift should be launched to develop low-energy information transmission (e.g., backscatter communication [1]) and reception, both facilitating implementation of low-energy IoT devices. Further, self-powering via energy harvesting should be devised [2]. Existing wireless power transfer (WPT) and simultaneous wireless information and power transfer (SWIPT) aim at enhancing the rate-energy tradeoff [3], [4], through optimum signal design for WPT and SWIPT on the one hand, and via implementation of appropriate receiver structure on the other, both at circuit and system levels.

Recent works on optimum signal design revealed that using multi-sine waveforms [5], [6] can bring considerable gain in the efficiency of WPT, compared to a single tone waveform. As for SWIPT, superposition of multi-sine waveforms and information-bearing signal (e.g., OFDM signal) effectively enhances the rate-energy tradeoff [7], given the deterministic energy signal can be eliminated before information decoding. These improvements resulted from building on a nonlinear model of the rectifier for energy harvesting, as clearly shown

Manuscript received September 1, 2016; accepted September 28, 2016. Date of publication September 30, 2016; date of current version December 15, 2016. This work was supported by the National Research Foundation of Korea (NRF) through the Korean Government (MSIP) under Grant 2014R1A5A1011478. The associate editor coordinating the review of this paper and approving it for publication was J. Coon.

The authors are with the School of Information and Communication Engineering, Sungkyunkwan University, Suwon 440-746, South Korea (e-mail: dikim@skku.ac.kr).

Digital Object Identifier 10.1109/LWC.2016.2614665

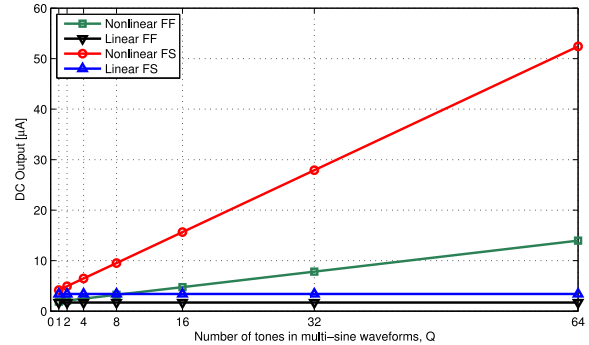


Fig. 1. DC output of the rectifier for a varying number of tones in multi-sine waveforms when its linear and nonlinear models are considered in frequency-flat (FF) and frequency-selective (FS) channels.

in Fig. 1, under which multi-sine waveforms with higher peak-to-average-power-ratios (PAPR) increase the DC output of the rectifier [6]. However, the superposition method causes undue power consumption for additional processing and conventional information decoding with I/Q down-conversion (i.e., mixer) and analog-to-digital conversion (ADC).

Recently, there has been the upsurge of interest in proposing specific receiver structures for SWIPT [8], [9], such as time switching (TS), power splitting (PS), antenna switching (AS), and integrated receiver (IntRx). The TS and PS are commonly used for simple realization and favorable rate-energy tradeoff, respectively. However, the far-field based RF energy harvesting is not sufficient enough to support conventional RF communications (e.g., OFDM and OFDM-IM) which require both I/Q down-conversion and ADC, as well as multiple antennas (e.g., AS) at a low-energy and low-complexity *passive* sensor node. For this reason, we do not consider the TS and PS followed by the I/Q down-conversion and ADC and also the AS which may not be suitable for use at the sensor node. Unlike other approaches, the IntRx is preferred for a combined receiver that performs RF-to-DC conversion at once, both for information decoding and energy harvesting, similar to the conversion in Fig. 2(b). But the IntRx with instantaneous received power for information decoding requires the channel estimation especially for fading channel. Also, the amplitude modulation is carried over a single tone waveform for the IntRx, which may not optimize the efficiency of WPT, unlike multi-sine waveforms.

Based on the above observations, we propose an innovative idea of using multi-sine waveforms for energy transfer and their distinct PAPR for information transmission, both through a single output of the rectifier. The latter performs the RF-to-DC conversion at once like the IntRx but does not require the

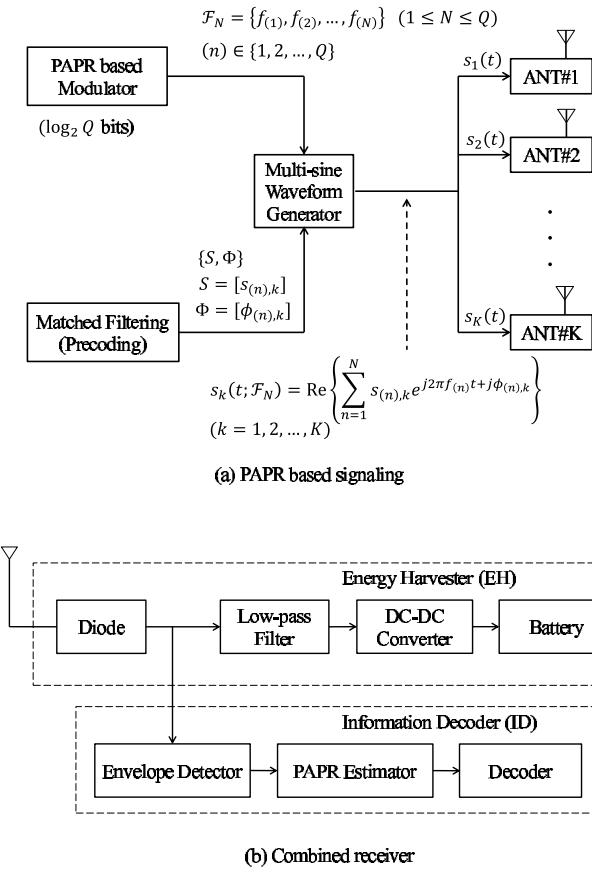


Fig. 2. New architecture for SWIPT using multi-sine waveforms for energy transfer and their distinct PAPR for information transmission. In the combined receiver (b), the time constant for envelope detection is shorter than that for low-pass filtering to yield the DC output.

channel estimation for information decoding. Thus, the information can be received with low-energy processing, instead of the high-energy processing of mixer and ADC. In this letter, we demonstrate how the proposed idea works by analyzing the performance of PAPR based information transmission for a varying number of tones in multi-sine waveforms and varying bandwidth. The latter would require the analysis for both frequency-flat (FF) and frequency-selective (FS) channels. It will be a key enabler for bringing low-energy IoT devices into reality which are capable of receiving the information with low energy and self-powering by the WPT with high efficiency, realizing eventual batteryless operation.

The remainder of this letter is organized as follows. Section II presents a new architecture for SWIPT using multi-sine waveforms and their distinct PAPR. In Section III, we consider the performance of the proposed SWIPT in terms of the bit-error rate and the rate-energy tradeoff, which is also compared with the IntRx with single tone and amplitude modulation. Concluding remarks are given in Section IV.

II. NEW ARCHITECTURE FOR SWIPT

A. Multi-Sine Waveforms and Transmit PAPR

The proposed architecture for SWIPT using multi-sine waveforms and their distinct PAPR is shown in Fig. 2. Here the information is conveyed by selecting a subset of the multi-sine

TABLE I
AN EXAMPLE MAPPING WHEN $Q = 4$

2 bits	N	$PAPR_{TX}$	\mathcal{F}_N
[0 0]	1	2	{ $f_{(1)}$ }
[0 1]	2	4	{ $f_{(1)}, f_{(2)}$ }
[1 0]	3	6	{ $f_{(1)}, f_{(2)}, f_{(3)}$ }
[1 1]	4	8	{ f_1, f_2, f_3, f_4 }

waveforms exhibiting a different level of PAPR as follows. Suppose there are Q tones available for SWIPT with minimum spacing Δf , which are given by

$$\mathcal{F} = \{f_1, f_2, \dots, f_Q\} \quad (1)$$

for $f_i = f_1 + (i - 1)\Delta f$, $i = 1, \dots, Q$. The subset $\mathcal{F}_N \subset \mathcal{F}$ is defined as

$$\mathcal{F}_N = \{f_{(1)}, f_{(2)}, \dots, f_{(N)}\} \quad (2)$$

where $(n) \in \{1, 2, \dots, Q\}$ for $1 \leq n \leq N$ and $(n) \neq (n')$ if $n \neq n'$. The $\log_2 Q$ -bit information can be one-to-one mapped to \mathcal{F}_N in an increasing order of $N = |\mathcal{F}_N| = 1, \dots, Q$, as shown in Table I. Note that all distinct subsets of same size N produce the same level of PAPR in (5) below, and \mathcal{F}_N acts as the *best* subset whose N tones undergo relatively better channel gains, especially for the FS channel.¹

Assume that an array of K multiple antennas is used at the transmitter for enhancing energy transfer efficiency. Then the multi-sine waveforms for the k th antenna, which are generated by the subset \mathcal{F}_N , can be expressed as

$$s_k(t; \mathcal{F}_N) = \operatorname{Re} \left\{ \sum_{n=1}^N s_{(n),k} \exp[j2\pi f_{(n)}t + j\phi_{(n),k}] \right\} \quad (3)$$

for $k = 1, \dots, K$. Here, $s_{(n),k}$ and $\phi_{(n),k}$ are the magnitude and initial phase associated with the (n) th tone $f_{(n)}$ at the k th antenna. Note that a total transmit power of P is allocated among K antennas as

$$\sum_{k=1}^K \mathbf{E} \left\{ |s_k(t; \mathcal{F}_N)|^2 \right\} \leq P \quad (4)$$

where \mathbf{E} denotes an expectation.

Now the $\log_2 Q$ -bit information is embedded into the *varying* peak-to-average-power-ratios (PAPR) of $s_k(t; \mathcal{F}_N)$ ($k = 1, \dots, K$) through the subset \mathcal{F}_N , which can be evaluated as

$$PAPR_{TX}^k(N) = \frac{\max_{t \in [0, T]} |s_k(t; \mathcal{F}_N)|^2}{\frac{1}{T} \int_T |s_k(t; \mathcal{F}_N)|^2 dt} \leq 2N. \quad (5)$$

It is to be noted that the upper bound on *transmit* PAPR, namely $PAPR_{TX} = 2N$ can be achieved with uniform power allocation among N tones and K antennas and all initial phases aligned, that is,

$$s_{(n),k} = \sqrt{\frac{2P}{NK}} \quad \text{and} \quad \phi_{(n),k} = \phi \quad \text{for } \forall n, k. \quad (6)$$

Thus, it is required to perform the matched-filtering (MF) while passing through the channel for amplitude matching and phase alignment at the receiver, which is addressed below.

¹This implies that the channel state information (CSI) will allow to select the *best* subset \mathcal{F}_N of N tones in a given transmission time.

B. Channel Model and Receive PAPR

The wireless charging of wearable devices and wireless sensors used to be performed in indoor channel environment, exhibiting a multi-path fading channel as

$$h_{(n),k}(t; \mathcal{F}_N) = \sum_{l=1}^L a_{(n),k,l} \exp(j\theta_{(n),k,l}) \delta(t - \tau_{(n),k,l}) \quad (7)$$

where $h_{(n),k}(t; \mathcal{F}_N)$ is the channel impulse response of the (n) th tone from the k th antenna, $a_{(n),k,l}$, $\theta_{(n),k,l}$ and $\tau_{(n),k,l}$ represent the corresponding channel gain, phase and delay associated with the l th path, respectively.

Since an array of K antennas is used for SWIPT, the received signal can be expressed as

$$r(t; \mathcal{F}_N) = \operatorname{Re} \left\{ \sum_{k=1}^K \sum_{n=1}^N s_{(n),k} w_{(n),k} \exp[j2\pi f_{(n)} t + j\phi_{(n),k}] \right\} + \eta(t). \quad (8)$$

Here $\eta(t)$ is the channel noise with zero mean and variance $N_o W$ for the signal bandwidth W and noise power spectral density level N_o . The composite complex-valued channel gain $w_{(n),k}$ (i.e., the sum of eigenvalues in channel response to a sinusoidal waveform) is given by

$$w_{(n),k} = \sum_{l=1}^L a_{(n),k,l} \exp(j\theta_{(n),k,l} - j2\pi f_{(n)} \tau_{(n),k,l}). \quad (9)$$

Here N tones in the subset \mathcal{F}_N are assumed to be spaced over a *selective* sub-band of the coherence bandwidth B_c (i.e., W), and $\{w_{(n),k}\}$ undergo similar Rayleigh-faded channel gains for different tones but appear independent for different antennas. We assume that the receiver sends a short pilot signal to the transmitter before each frame transmission to estimate the composite channel gains $\{w_{(n),k}\}$, provided the channel reciprocity holds in the frame transmission for SWIPT.

To achieve the higher energy transfer efficiency and also the upper bound of transmit PAPR, we assume that the transmitter performs the MF (i.e., precoding) for the amplitude matching and phase alignment at the receiver. Therefore, the complex envelope of the (n) th tone in the multi-sine waveforms for the k th antenna should be adjusted as

$$s_{(n),k} \exp(j\phi_{(n),k}) = \sqrt{2P} \frac{w_{(n),k}^*}{\sqrt{\sum_{k=1}^K \sum_{n=1}^N |w_{(n),k}|^2}} \quad (10)$$

where $(\cdot)^*$ denotes complex conjugate and the transmit power constraint in (4) has been applied. Using the channel vector $\mathbf{w}_{(n)} = [w_{(n),1}, w_{(n),2}, \dots, w_{(n),K}]$, the received signal in (8) after the precoding can be simplified to

$$r(t; \mathcal{F}_N) = \sqrt{\frac{2P}{\sum_{n=1}^N \|\mathbf{w}_{(n)}\|^2}} \sum_{n=1}^N \|\mathbf{w}_{(n)}\|^2 \cos(2\pi f_{(n)} t) + \eta(t). \quad (11)$$

At the receiver, the rectifier in Fig. 2(b) performs the RF-to-DC conversion and follows the envelope of the received signal

in (11), based upon which the *receive* PAPR is measured as

$$\begin{aligned} PAPR_{RX}(N) &= \frac{\max_{t \in [0, T]} |r(t; \mathcal{F}_N)|^2}{\frac{1}{T} \int_T |r(t; \mathcal{F}_N)|^2 dt} \\ &\approx \frac{\left| \sqrt{2P \sum_{n=1}^N \|\mathbf{w}_{(n)}\|^2} + \eta \right|^2}{\frac{P \sum_{n=1}^N \|\mathbf{w}_{(n)}\|^4}{\sum_{n=1}^N \|\mathbf{w}_{(n)}\|^2} + N_o B_c}. \end{aligned} \quad (12)$$

If the channel noise can be ignored, given the received power level is -10dBm for energy signal, unlike -60dBm for information signal, the receive PAPR reduces to

$$PAPR_{RX}(N) \approx \frac{2 \left(\sum_{n=1}^N \|\mathbf{w}_{(n)}\|^2 \right)^2}{\sum_{n=1}^N \|\mathbf{w}_{(n)}\|^4}. \quad (13)$$

Moreover, if the channel appears frequency flat (FF), namely $\mathbf{w}_{(n)} = \mathbf{w}$ for $\forall n$, then the receive PAPR achieves the upper bound as

$$PAPR_{RX}(N) \approx \frac{2N \|\mathbf{w}\|^4}{\|\mathbf{w}\|^4} = 2N. \quad (14)$$

It is of paramount importance that the receive PAPR can achieve the upper bound $PAPR_{RX} = PAPR_{TX} = 2N$ regardless of the channel vector $\mathbf{w}_{(n)}$, which implies that the energy transfer efficiency can be maximized with the *MF* (i.e., precoding) at the transmitter, while the upper bound on transmit PAPR being achieved at the receiver.

Especially, the channel estimation is not required at the receiver for the PAPR based information decoding in such FF channel. Even if the channel appears frequency selective (FS), we can identify a sub-band with higher channel gain over which it appears FF, thereby no channel estimation.

III. PERFORMANCE CONSIDERATIONS

A. Bit-Error Rate (BER)

To validate the proposed idea of information transmission using distinct PAPR, the bit-error rate (BER) is evaluated as

$$P_b(N) = 1 - \Pr[2N - 1 \leq PAPR_{RX}(N) \leq 2N + 1] \quad (15)$$

for $2 \leq N \leq Q - 1$, and

$$P_b(N) = \begin{cases} \Pr[PAPR_{RX}(N) \geq 3] & \text{for } N = 1, \\ 1 - \Pr[PAPR_{RX}(N) \geq 2Q - 1] & \text{for } N = Q. \end{cases} \quad (16)$$

Fig. 3 shows the BER performance versus average received signal-to-noise ratio (SNR) for $K = 1$ when both FF and FS channels are considered with bandwidth $B_T = 1\text{MHz}$ and 10MHz , respectively. In the FS channel, we have identified the sub-band of $B_c = 1\text{MHz}$ over which the FF channel appears, and the PAPR based information transmission was performed over this sub-band. Here, the numerical BER evaluations based on (12), (15) and (16) are validated by Monte Carlo simulations. Further, the BER performance of the multi-sine waveforms ($Q = 16$) with PAPR based information decoding is compared with that of the single carrier ($Q = 1$) with $M = 16$ -ary PAM signaling (i.e., instantaneous received power for information decoding). We observe that their BER performance is comparable in the SNR range of interest.

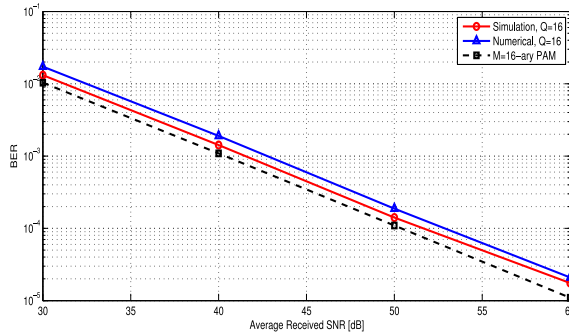


Fig. 3. BER versus average received SNR for PAPR based signaling with $Q = 16$ tones and single carrier with $M = 16$ -ary PAM signaling.

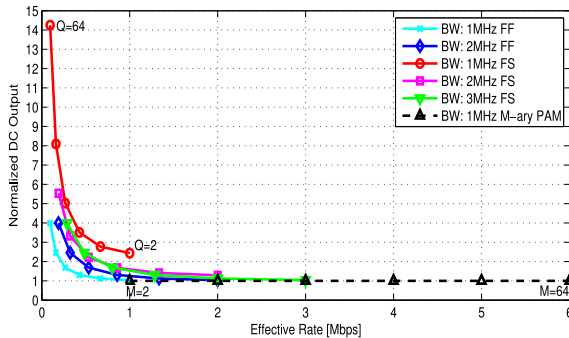


Fig. 4. Rate-energy tradeoff for varying Q and M in multi-sine waveforms with PAPR and single carrier with M -ary PAM, respectively.

B. Rate-Energy Tradeoff

The multi-sine waveforms for SWIPT are generated with the minimum spacing $\Delta f = T^{-1}$ for the symbol time T . Hence, if we define the coherence bandwidth $B_c \ll B_T$ as a sub-band with higher channel gain in FS channel, the information rate can be evaluated as

$$R_b = \frac{1}{T} \log_2(1 + B_c T) \quad \text{bits/sec} \quad (17)$$

for $Q = 1 + B_c T$. We observe that as the number of tones available Q increases, the harvested energy offered by multi-sine waveforms is increased, referring to [6]

$$\text{DC Output} = \frac{1}{Q} \sum_{N=1}^Q \left(C_2 P_r + C_4 \frac{2N^2 + 1}{2N} P_r^2 \right) \quad (18)$$

for the received power P_r , constants C_2 and C_4 when $K = 1$. But the symbol time T in (17) is also increased with fixed B_c , resulting in reduced information rate. Therefore, there exists a rate-energy tradeoff for varying Q by which proper selection of B_c can be made, considering a specific channel gain offered by a sub-band within B_T in the FS channel [6].

In Fig. 4, the DC output with the single carrier ($Q = 1$) is normalized to one while the achievable data rate is increasing with $M = 2, 4, 8, 16, 32, 64$, subject to the target BER of 10^{-3} . Note that the data rate of the single carrier with M -ary PAM signaling is set to $R_b = B_c \frac{\log_2 M}{1+\beta}$ for the roll-off factor β , which is assumed to be zero for the minimum Nyquist bandwidth of $B_c = 1\text{MHz}$, whose BER performance is maintained below the target BER for all M above. This is

because the energy signal of $P_r = -20\text{dBm}$ produces the higher SNR of 50dB when the effective noise level is typically -130dBm/Hz over the sub-band of 1MHz. The proposed SWIPT using multi-sine waveforms and PAPR provides much higher normalized DC output relative to the single carrier ($Q = 1$) with $Q = 2, 4, 8, 16, 32, 64$ in (18), though the data rate in (17) is decreasing but still acceptable for the low-rate IoT sensor applications. In this situation, the coverage of RF energy transfer to a sensor node is the most critical which can be greatly enlarged with the proposed SWIPT.

Therefore, the proposed SWIPT trade-offs the data rate for the far increased coverage of RF energy transfer, which is desired for use in the SWIPT downlink to a low-energy and low-complexity *passive* sensor node. In Fig. 4, we see that the proposed SWIPT with $Q = 2$ provides a higher harvested energy than the single carrier with $M = 2$, while achieving the same data rate with comparable BER performance, beyond which the trade-off occurs to increase the coverage.

IV. CONCLUSION

In this letter we have implemented a new form of SWIPT using the PAPR based signaling and combined receiver that realizes the RF-to-DC conversion at once, both for information decoding and energy harvesting, and the former does not require the channel estimation. Especially, the PAPR based information transmission over a selective sub-band offers the reliable BER performance regardless of its specific channel gain, as long as the sub-band appears frequency-flat (FF) channel. Using multi-sine waveforms was shown to be the prerequisite for efficient WPT, and in conjunction with PAPR based information decoding, it leads to a promising solution for realizing low-energy IoT sensors. This will be a key enabler for bringing their batteryless operation into reality, expecting the massive and dense deployment of machine-type communication (MTC) for IoT sensor applications.

REFERENCES

- [1] V. Liu *et al.*, "Ambient backscatter: Wireless communication out of thin air," in *Proc. ACM SIGCOMM*, Hong Kong, Aug. 2013, pp. 39–50.
- [2] X. Lu, P. Wang, D. Niyato, D. I. Kim, and Z. Han, "Wireless networks with RF energy harvesting: A contemporary survey," *IEEE Commun. Surveys Tuts.*, vol. 17, no. 2, pp. 757–789, 2nd Quart., 2015.
- [3] S. Bi, C. K. Ho, and R. Zhang, "Wireless powered communication: Opportunities and challenges," *IEEE Commun. Mag.*, vol. 53, no. 4, pp. 117–125, Apr. 2015.
- [4] K. Huang and X. Zhou, "Cutting the last wires for mobile communications by microwave power transfer," *IEEE Commun. Mag.*, vol. 53, no. 6, pp. 86–93, Jun. 2015.
- [5] A. S. Boaventura and N. B. Carvalho, "Maximizing DC power in energy harvesting circuits using multisine excitation," in *IEEE MTT-S Int. Microwave Symp. Dig. (MTT)*, Baltimore, MD, USA, Jun. 2011, pp. 1–4.
- [6] B. Clerckx and E. Bayguzina, "Waveform design for wireless power transfer," *arXiv:1604.00074*.
- [7] B. Clerckx, "Waveform optimization for SWIPT with nonlinear energy harvester modeling," *arXiv:1602.01061*.
- [8] R. Zhang and C. K. Ho, "MIMO broadcasting for simultaneous wireless information and power transfer," *IEEE Trans. Wireless Commun.*, vol. 12, no. 5, pp. 1989–2001, May 2013.
- [9] X. Zhou, R. Zhang, and C. K. Ho, "Wireless information and power transfer: Architecture design and rate-energy tradeoff," *IEEE Trans. Commun.*, vol. 61, no. 11, pp. 4754–4767, Nov. 2013.